Synthesis and Molecular Structures of Perfluoro-*n*-alkyl Complexes of Platinum(II) and Platinum(IV) Containing Tetramethylethylenediamine (TMEDA) or 1,2-Bis(diphenylphosphino)ethane (DPPE) Ligands

Russell P. Hughes,*[,†] Joel T. Sweetser,[†] Mark D. Tawa,[†] Alex Williamson,[†] Christopher D. Incarvito,[‡] Brian Rhatigan,[‡] Arnold L. Rheingold,[‡] and Gene Rossi[‡]

Departments of Chemistry, 6128 Burke Laboratory, Dartmouth College, Hanover, New Hampshire 03755, and University of Delaware, Newark, Delaware 19716

Received May 21, 2001

Reaction of (TMEDA)Pt(CH_3)$_2$ with *n*-perfluoropropyl iodide in hexanes results in an apparent *cis* addition of the perfluoroalkyl iodide to give the six-coordinate Pt(IV) complex (TMEDA)Pt(*n*-C_3F_7)(CH_3)$_2$I (**6a**). Complex **6a** slowly and reversibly reductively eliminates CH_3I in solution to afford an equilibrium with the Pt(II) complex (TMEDA)Pt(*n*-C_3F_7)(CH_3) (**9a**). Addition of triethylamine drives the equilibrium toward **9a**. Identical reactions of perfluoroethyl iodide are observed to afford **6b** and **9b**. Reaction of **6a** with $AgBF_4$ generates the cationic Pt(IV) complex [(TMEDA)Pt(*n*-C_3F_7)(CH_3)$_2$(OH_2)]BF_4 (**11**), which reacts with NaCl to form (TMEDA)Pt(*n*-C_3F_7)(CH_3)$_2$Cl (**12**); both reactions retain the *cis* stereochemistry of the starting material **6a**. Reaction of **9a** with CF_3SO_3H in moist solvents generates the cationic Pt(II) complex [(TMEDA)Pt(*n*-C_3F_7)(OH_2)]O_3SCF_3 (**17**), which reacts with iodide to afford the neutral iodide complex (TMEDA)Pt(*n*-C_3F_7)I (**14**). Reaction of complex **9a** with I_2 in hexanes results in *trans* addition of I_2 to generate (TMEDA)Pt(C_3F_7)(CH_3)I_2 (**13**), which is converted to (TMEDA)Pt(*n*-C_3F_7)I (**7**) by treatment with $AgBF_4$ followed by NaI. Complex **14** reacts with $NaBH_4$ to produce (TMEDA)Pt(*n*-C_3F_7)H (**18**). The TMEDA ligand can be displaced from **9a** by DPPE to give (DPPE)Pt(*n*-C_3F_7)(CH_3) (**19**), which reacts with CF_3-SO_3H to give the triflate complex (DPPE)Pt(*n*-C_3F_7)O_3SCF_3 (**20**), in equilibrium with a water complex, [(DPPE)Pt(*n*-C_3F_7)(OH_2)]O_3SCF_3 (**21**). Reaction of **20** with iodide, or **19** with I_2, gives (DPPE)Pt(*n*-C_3F_7)I (**22**), which can be converted to the hydrido complex (DPPE)Pt(*n*-C_3F_7)H (**23**) with $NaBH_4$. The X-ray crystal structures of complexes **6a**, **9a**, **9b**, **10**, **13**, **18**, **19**, **20**, and **23** have been determined, and structural comparisons in terms of ligand *cis* and *trans* influences are discussed.

Introduction

The oxidative addition reaction of an alkyl halide to a metal center is among the most useful methods of forming a new metal−carbon bond.[1] As a result of a recent renaissance of interest in the chemistry of fluoroalkyl ligands, involving F-migrations to and from metal centers[2,3] and activation of carbon−fluorine bonds by hydrolysis,[4] hydrogenolysis,[5] or hydride reagents,[6] we have been interested in reevaluating and expanding some of the previously reported methodology for the synthesis of late metal−fluoroalkyl complexes. Many such complexes have also been reported using oxidative addition methodology, usually involving perfluoroalkyl iodides,[7−12] but we have shown previously that this route can be problematical for both early and late metals due to fluoroalkylation at ligand sites, rather than at the metal center.[13−16]

There have been many studies of oxidative additions of alkyl halides to square planar Pt(II) precursors.[17−21] In most cases, reactions of primary alkyl iodides and

† Dartmouth College.
‡ University of Delaware.

(1) Collman, J. P.; Hegedus, L. S.; Norton, J. R.; Finke, R. G. *Principles and Applications of Organotransition Metal Chemistry*; University Science Books: Mill Valley, CA, 1987.
(2) Huang, D.; Koren, P. R.; Folting, K.; Davidson, E. R.; Caulton, K. G. *J. Am. Chem. Soc.* **2000**, *122*, 8916−8931.
(3) Huang, D.; Caulton, K. G. *J. Am. Chem. Soc.* **1997**, *119*, 3185−3186.
(4) Hughes, R. P.; Lindner, D. C.; Rheingold, A. L.; Liable-Sands, L. M. *J. Am. Chem. Soc.* **1997**, *119*, 11544−11545.
(5) Hughes, R. P.; Smith, J. M. *J. Am. Chem. Soc.* **1999**, *121*, 6084−6085.
(6) Draft, B. M.; Lachicotte, R. J.; Jones, W. D. *J. Am. Chem. Soc.* **2000**, *122*, 8559−8560.
(7) McCleverty, J. A.; Wilkinson, G. *J. Chem. Soc.* **1964**, 4200−4203.
(8) Rosevear, D. T.; Stone, F. G. A. *J. Chem. Soc. A* **1968**, 164−167.
(9) Mukhedkar, A. J.; Green, M.; Stone, F. G. A. *J. Chem. Soc. (A)* **1969**, 3023−3026.
(10) Stone, F. G. A. *Endeavour* **1966**, *25*, 33−38.
(11) Clark, H. C.; Manzer, L. E. *J. Organomet. Chem.* **1973**, *59*, 411−428.
(12) Appleton, T. G.; Hall, J. R.; Kennard, C. H. L.; Mathieson, M. T.; Neale, D. W.; Smith, G.; Mak, T. C. W. *J. Organomet. Chem.* **1993**, *453*, 299−306.
(13) Hughes, R. P.; Maddock, S. M.; Guzei, I. A.; Liable-Sands, L. M.; Rheingold, A. L. *J. Am. Chem. Soc.* **2001**, *123*, 3279−3288.
(14) Hughes, R. P.; Husebo, T. L.; Holliday, B. J.; Rheingold, A. L.; Liable-Sands, L. M. *J. Organomet. Chem.* **1997**, *548*, 109−112.
(15) Hughes, R. P.; Maddock, S. M.; Rheingold, A. L.; Liable-Sands, L. M. *J. Am. Chem. Soc.* **1997**, *119*, 5988−5989.
(16) Hughes, R. P.; Husebo, T. L.; Rheingold, A. L.; Liable-Sands, L. M.; Yap, G. P. A. *Organometallics* **1997**, *16*, 5−7.

10.1021/om010424h CCC: $20.00
Publication on Web 07/26/2001

bromides with dimethyl platinum(II) complexes occur by a polar S_N2 mechanism to give a Pt(IV) complex with kinetically controlled *trans* stereochemistry,[18] although *cis* products have been shown to result from subsequent isomerization.[22] On occasion, cationic five-coordinate intermediates have been detected spectroscopically.[23] Not surprisingly, the five-coordinate intermediate in the oxidative addition reaction has also been shown to serve as the key intermediate for reductive elimination of methyl iodide or ethane from Pt(IV).[24−26]

While most studies of oxidative addition/reductive elimination to Pt(II) have involved complexes bearing monodentate or bidentate phosphorus ligands, compounds with chelating nitrogen ligands have also been examined.[18] *cis*-Dialkyl and -diarylplatinum(II) complexes with nitrogen-donor ligands usually react with alkyl halides to give the *trans* oxidative addition product,[27−30] while the corresponding *cis* isomer can be formed either by competitive *cis* oxidative addition pathways or by *trans* oxidative addition with subsequent isomerization of the platinum(IV) product to a thermodynamically more stable *cis* isomer.[18] Dimethylplatinum(II) complexes containing pyridine,[27] 2,2′-bipyridine,[31] 1,10-phenanthroline,[31,32] and tetramethylethylenediamine (TMEDA) ligands[33,34] have been studied. For example, reaction of (TMEDA)Pt$(CH_3)_2$ (**1**) with benzyl bromide affords the *trans* addition product **2**.[33]

Fluoroalkyl complexes of platinum have also been approached in a similar fashion. For example, (COD)Pt$(CH_3)_2$ reacts with CF_3I to give (COD)Pt$(CF_3)_2$ with $[Pt(CH_3)_3I]_4$ as a byproduct;[11] subsequently the mixed alkyl compound (COD)Pt$(CH_3)(CF_3)$ was also identified as a product,[12] and (NBD)Pt$(CH_3)_2$ was shown to afford (NBD)Pt$(CH_3)(CF_3)$ and (NBD)Pt$(CF_3)_2$.[12] Reactions with perfluoroethyl, perfluoropropyl, and perfluoroisopropyl iodides apparently formed stable platinum(II) complexes, though none could be isolated in pure form.[11] These products are all presumed to result from facile reductive elimination from a platinum(IV) intermediate.

Recently, we described the reactions of perfluoroalkyl iodides with (TMEDA)Pd$(CH_3)_2$ to give square planar fluoroalkyl complexes **3** and **4**.[35] These reactions were also assumed to proceed via oxidative addition to give an unobserved Pd(IV) intermediate, followed by reductive elimination to give the Pd(II) product. Products **3** and **4** exhibited interesting structural parameters and variable-temperature NMR behavior, and we were interested in preparing their Pt(II) analogues for comparison and to see if we could observe Pt(IV) intermediates en route to their formation. Accordingly, we have studied the corresponding reactions of the platinum analogue **1** with various fluoroalkyl iodides.

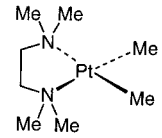

1

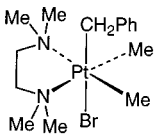

2

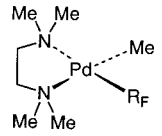

3

a. $R_F = CF_2CF_2CF_3$
b. $R_F = CF_2CF_2CF_2CF_3$
c. $R_F = CF(CF_3)_2$

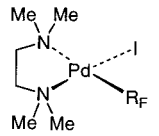

4

a. $R_F = CF_2CF_2CF_3$
b. $R_F = CF_2CF_2CF_2CF_3$
c. $R_F = CF(CF_3)_2$

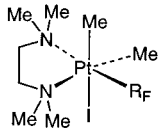

6a. $R_F = CF_2CF_2CF_3$
6b. $R_F = CF_2CF_3$

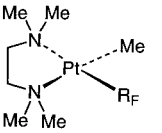

9a. $R_F = CF_2CF_2CF_3$
9b. $R_F = CF_2CF_3$

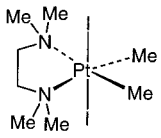

10

Results and Discussion

Perfluoroalkyl Pt(IV) and Pt(II) Complexes with TMEDA Ligands. When a suspension of **1** in hexanes is treated with *n*-C_3F_7I, the starting material rapidly dissolves to form a yellow solution, from which a white solid slowly precipitates in excellent yield. The ^1H NMR spectrum of the product is consistent with a Pt(IV) adduct, (TMEDA)Pt$(C_3F_7)(CH_3)_2I$, exhibiting four distinct NMe resonances and two separate PtMe signals. The ^{19}F NMR spectrum shows each pair of fluorines in the CF_2 groups to be diastereotopic; the two α-CF_2 fluorine resonances are well separated (by 16.5 ppm), show a large geminal coupling constant, $^2J_{FF} = 257$ Hz,

(17) Ellis, P. R.; Pearson, J. M.; Haynes, A.; Adams, H.; Bailey, N. A.; Maitlis, P. M. *Organometallics* **1994**, *13*, 3215−3226.
(18) Rendina, L. M.; Puddephatt, R. J. *Chem. Rev.* **1997**, *97*, 1735−1754.
(19) Jawad, J. K.; Puddephatt, R. J. *J. Chem. Soc., Dalton Trans.* **1977**, 1466−1469.
(20) Jawad, J. K.; Puddephatt, R. J. *J. Organomet. Chem.* **1976**, *117*, 297−302.
(21) Scott, J. D.; Puddephatt, R. J. *Organometallics* **1986**, *5*, 1538−1544.
(22) Felice, V. D.; Giovannitti, B.; Renzi, A. D.; Tesauro, D.; Penunzi, A. *J. Organomet. Chem.* **2000**, *593−594*, 445−453.
(23) Crespo, M.; Puddephatt, R. J. *Organometallics* **1987**, *6*, 2548−2550.
(24) Brown, M. P.; Puddephatt, R. J.; Upton, C. E. E. *J. Chem. Soc., Dalton Trans.* **1974**, 2457−2465.
(25) Goldberg, K. I.; Yan, J.; Breitung, E. M. *J. Am. Chem. Soc.* **1995**, *117*, 6889−6896.
(26) Goldberg, K. I.; Yan, J. Y.; Winter, E. L. *J. Am. Chem. Soc.* **1994**, *116*, 1573−1574.
(27) Appleton, T. G.; Hall, J. R.; Williams, M. A. *J. Organomet. Chem.* **1986**, *303*, 139−149.
(28) Aye Khin, T.; Canty, A. J.; Crespo, M.; Puddephatt, R. J.; Scott, J. D.; Watson, A. A. *Organometallics* **1989**, *8*, 1518−1522.
(29) Byers, P. K.; Canty, A. J.; Crespo, M.; Puddephatt, R. J.; Scott, J. D. *Organometallics* **1988**, *7*, 1363−1367.
(30) Arsenault, G. J.; Crespo, M.; Puddephatt, R. J. *Organometallics* **1987**, *6*, 2255−2256.
(31) Monaghan, P. K.; Puddephatt, R. J. *Organometallics* **1984**, *3*, 444−449.
(32) Monaghan, P. K.; Puddephatt, R. J. *Organometallics* **1985**, *4*, 1406−1412.
(33) Graaf, W. d.; Boersma, J.; Koten, G. v. *Organometallics* **1990**, *9*, 1479−1484.
(34) Prokopchuck, E. M.; Jenkins, H. A.; Puddephatt, R. J. *Organometallics* **1999**, *18*, 2861−2866.
(35) Hughes, R. P.; Overby, J. S.; Williamson, A.; Lam, K.-C.; Concolino, T. E.; Rheingold, A. L. *Organometallics* **2000**, *19*, 5190−5201.

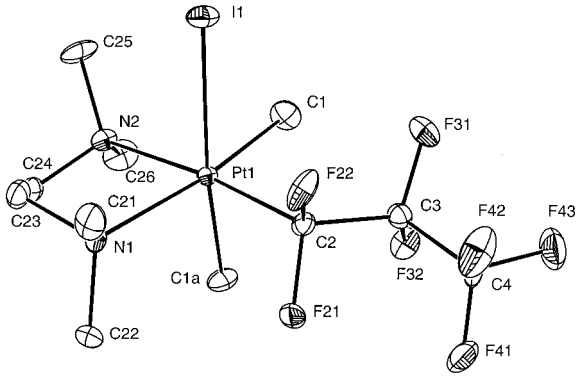

Figure 1. ORTEP diagram of the non-hydrogen atoms of **6a**, showing atom-labeling scheme. Thermal ellipsoids are shown at the 30% level.

and also couple to Pt with different coupling constants ($^2J_{F1Pt} = 300$ Hz, $^2J_{F2Pt} = 251$ Hz). These data indicate that the product possesses no symmetry and are inconsistent with a *trans* adduct of structure **5**, (Scheme 1) in contrast to the reactions of the bis(dimethylphosphino)ethane analogue of **1** with fluoroalkyl iodides, which do give analogous *trans* adducts.[36] Of the two possible *cis* adducts, structure **6a** is confirmed by a single-crystal X-ray diffraction study (see below) and is assumed to be the solution structure. An ORTEP of the structure of **6a** is shown in Figure 1. Details of the crystallographic determinations of all compounds in this paper are presented in Table 1, and discussion of structural details is deferred until later. An analogous reaction occurs with C_2F_5I to afford the perfluoroethyl complex **6b**.

The oxidative addition reactions of fluoroalkyl iodides to transition metals are unlikely to proceed via a polar S_N2 attack by the metal at carbon, due to the unfavorable polarity of the $C^{\delta-}-I^{\delta+}$ bond.[37,38] In previous systems involving reactions of primary perfluoroalkyl iodides we have postulated that these reactions proceed via electron transfer to the fluoroalkyl iodide, followed by rapid loss of iodide from the resultant radical anion, and very fast trapping of the fluoroalkyl radical at the metal.[13,16] An analogous pathway in this case, shown in Scheme 1 using perfluoro-*n*-propyl iodide, would proceed via intermediate **7**, which is indistinguishable from that obtained by nucleophilic displacement at carbon. Subsequent trapping of **7** by iodide would give **5**, which is not observed, or **7** could undergo a rearrangement to **8** followed by trapping by iodide to afford the observed product **6**. Alternatively, the observed *cis* stereochemistry may be the result of an initial, perhaps concerted, *cis* oxidative addition or might be obtained by initial *trans* oxidative addition to give **5**, followed by *cis* reductive elimination of CH_3I to form **9a**, which then undergoes *trans* oxidative addition of CH_3I to form complex **6a**. However, the latter sequence appears to violate the principle of microscopic reversibility in requiring a different stereochemistry for reductive elimination and oxidative addition of CH_3I. In addition,

Table 1. Crystal Data and Summary of X-ray Data Collection

	6a	**9a**	**9b**	**10**	**13**	**18**	**19**	**20**	**23**
formula	$C_{11}H_{22}F_7IN_2Pt$	$C_{10}H_{19}F_7N_2Pt$	$C_9H_{19}F_5N_2Pt$	$C_8H_{22}I_2N_2Pt$	$C_{10}H_{19}F_7I_2N_2Pt$	$C_9H_{17}F_7N_2Pt$	$C_{30}H_{27}F_7P_2Pt$	$C_{30}H_{24}F_{10}O_3P_2PtS$	$C_{29}H_{25}F_7P_2Pt$
fw	637.30	495.36	445.35	595.17	749.16	481.34	777.55	911.58	763.52
space group	*Pbca*	*P*1	*P*2(1)/*n*	*C*2/*c*	*P*2(1)/*n*	*P*2(1)/*c*	*P*2(1)/*n*	*P*2(1)/*n*	*P*2(1)/*c*
a, Å	8.6369(6))	8.471(10)	11.6898(8)	7.8250(11)	9.1644(11)	8.5383(5)	11.4958(13)	12.1620(8)	17.867(2)
b, Å	15.2123(10	9.017(6	8.6887(5)	13.7115(18)	17.094(2)	20.3171(12)	16.647(3)	15.9726(10	10.1868(12)
c, Å	26.0683(16)	9.972(9)	13.7432(9)	13.4113(17)	11.4330(14)	8.3699(5)	15.675(2)	16.7558(11)	31.964(4)
α, deg	90	90.62(6)	90	90	90	90	90	90	90
β, deg	90	94.02(9)	106.6140(10)	104.217(2)	93.837(2)	105.0150(10)	104.413(12)	104.6000(10)	103.467(2)
γ, deg	90	99.40(6)	90	90	90	90	90	90	90
V, Å^3	3425.0(4)	749.5(12)	1337.61(15)	1394.9(3)	1787.0(4)	1402.38(14)	2905.4(7)	3149.9(4)	5657.6(11)
Z	8	2	4	4	4	4	4	4	8
D (calcd), g/cm^3	2.472	2.195	2.211	2.834	2.785	2.280	1.778	1.922	1.793
abs coeff, mm^{-1}	10.060	9.427	10.530	14.454	11.368	10.073	5.003	4.714	5.137
temp, K	173(2)	241(2)	173(2)	173(2)	173(2)	173(2)	253(2)	293(2)	173(2)
diffractometer					Siemens P4				
radiation					Mo Kα 0.71073 Å				
R(*F*), %[a]	3.67	7.06	2.30	5.27	4.12	6.37	3.64	3.22	5.91
$R(wF^2)$, %[a]	11.92	15.32	5.76	15.53	13.91	20.05	8.07	10.01	11.98

[a] Quantity minimized = $R(wF^2) = \sum[w(F_o^2 - F_c^2)^2]/\sum[(wF_o^2)^2]^{1/2}$; $R = \sum\Delta/\sum(F_o)$, $\Delta = |(F_o - F_c)|$.

(36) Hughes, R. P.; Sweetser, J. T.; Williamson, A.; Incarvito, C. D.; Lam, K.-C.; Rheingold, A. L. Manuscript in preparation.

(37) Wakselman, C.; Lantz, A. In *Organofluorine Chem*; Banks, R. E., Smart, B. E., Tatlow, J. C., Eds.; Plenum: New York, NY, 1994; pp 177−194.

(38) Wakselman, C. *J. Fluorine Chem.* **1992**, *59*, 367−378.

Scheme 1

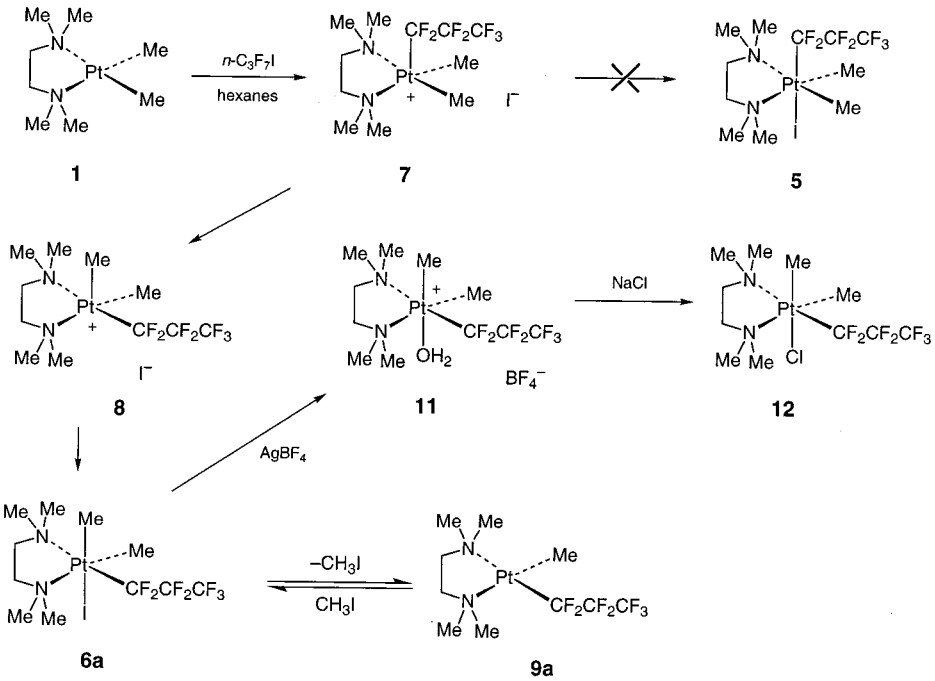

9a, which can be prepared independently (see below), is virtually insoluble in hexane, and treatment of a suspension of **9a** with CH_3I results in no reaction, although the reaction to form **6a** proceeds smoothly in $CDCl_3$ solution. Consequently, the intermediacy of **9a** in the formation of **6a** in hexanes seems unlikely. Fortunately, the low solubility of complex **6a** in hexanes precludes it from undergoing further reactions (see below) and allows it to be isolated in excellent yields.

On dissolution of complex **6a** in acetone, CH_2Cl_2, $CHCl_3$, or toluene at room temperature, slow reversible reductive elimination of CH_3I occurs and an equilibrium mixture of **6a** and **9a** is obtained after 24 h. The equilibrium constant, measured at 21 °C, is 0.015 in acetone-d_6 or $CDCl_3$ and 0.008 in toluene-d_8. This reaction presumably involves dissociation of iodide from **6a**, followed by nucleophilic attack of iodide on the axial methyl group of intermediate **8**, i.e., the microscopic reverse of the expected pathway for oxidative addition of CH_3I to **9a**. Addition of excess Et_3N to the equilibrium mixture affords, after several hours, complete conversion to $[Et_3NMe]I$ and **9a**, which was isolated and characterized by spectroscopic and crystallographic methods (see below). The role of Et_3N may be to shift the equilibrium by reacting with eliminated CH_3I to produce $[Et_3NMe]I$, or it may directly attack a methyl ligand in cationic intermediate **8**. We have no evidence to distinguish between these possibilities in this system, but observations outlined later suggest the latter pathway. While no reaction between **9a** and excess CH_3I is observed in hexanes, addition of excess CH_3I to a solution of **9a** in $CDCl_3$ affords complete conversion to **6a** within 4 h, thereby confirming the stereochemistry of oxidative addition of CH_3I to **9a** and, by microscopic reversibility, the stereochemistry of reductive elimination from **6a**.

A similar equilibrium occurs with **6b**, which can be cleanly transformed to the Pt(II) compound **9b** using NEt_3 in refluxing acetone. Complex **9b** was also characterized crystallographically. An ORTEP of the structure of **9a** is provided in Figure 2, and that of **9b** in Figure 3; details of the structures are discussed later.

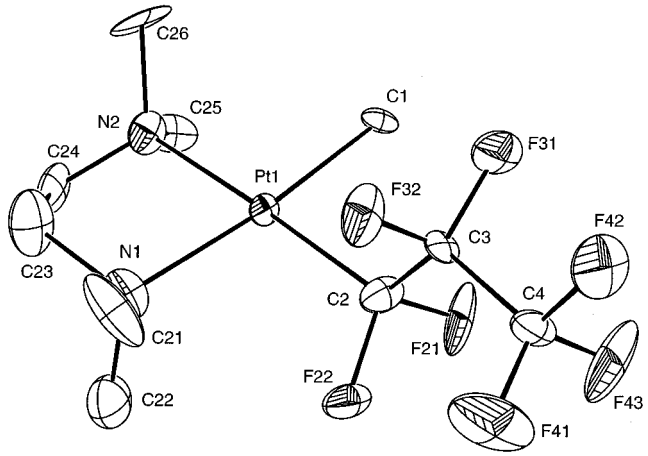

Figure 2. ORTEP diagram of the non-hydrogen atoms of **9a**, showing atom-labeling scheme. Thermal ellipsoids are shown at the 30% level.

In contrast to the clean reaction in hexanes, treatment of **1** with *n*-C_3F_7I in THF solution affords a mixture of several products. Compounds **9a** and **10** were identified as components of this mixture, but could only be isolated in small quantities using this method; the best route to **9a** is via **6a** as described above. Complex **10** contains no fluorinated ligand, and we have made no attempts to identify its rather murky origins, but an ORTEP of its structure is provided in Figure 4; details of the structure are discussed later.

Attempts to prepare an analogue of the putative cationic Pt(IV) intermediate **8** by treatment of **6a** with $AgBF_4$ in toluene afforded a yellow solid **11** after workup that appears to contain a water molecule in the sixth coordination site; inclusion of a molecule of water generates C and H percentages that agree well with the experimental data, while omission of the water molecule

Scheme 2

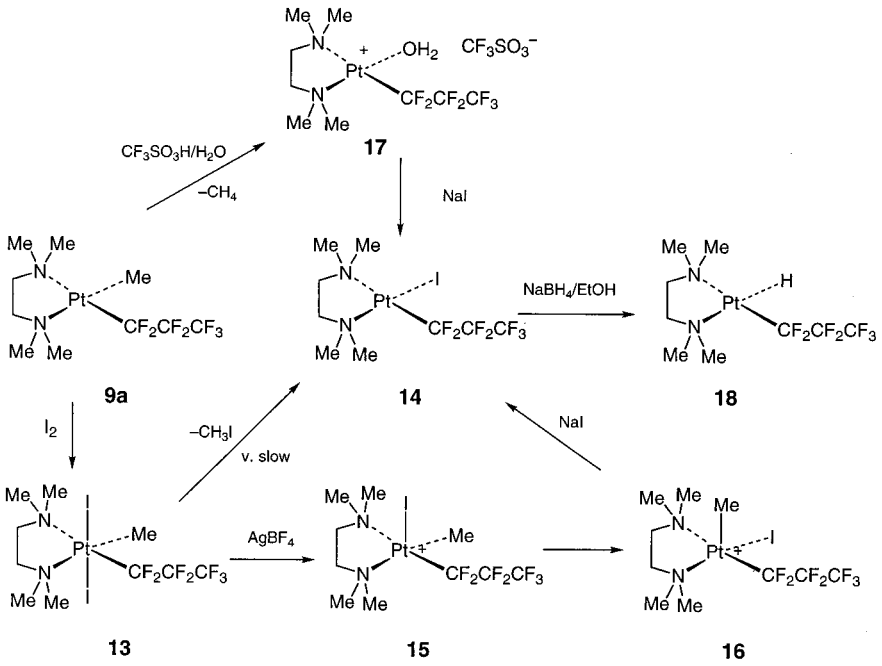

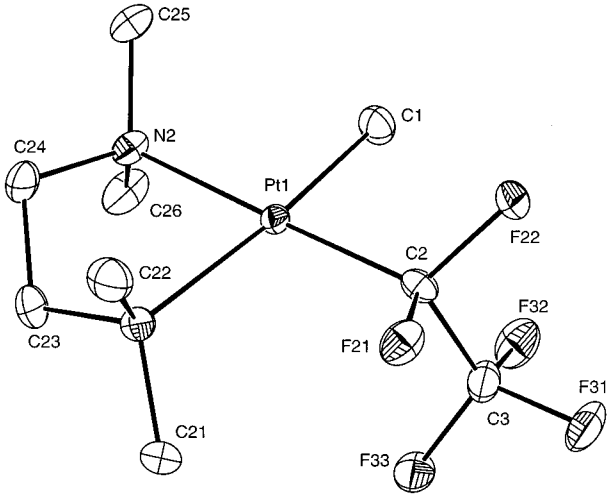

Figure 3. ORTEP diagram of the non-hydrogen atoms of **9b**, showing atom-labeling scheme. Thermal ellipsoids are shown at the 30% level.

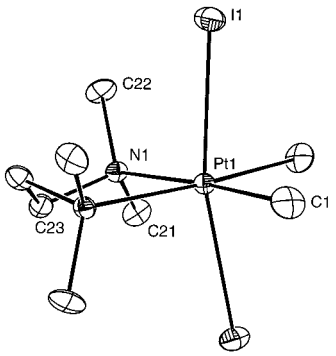

Figure 4. ORTEP diagram of the non-hydrogen atoms of **10**, showing atom-labeling scheme. Thermal ellipsoids are shown at the 30% level.

puts the values outside acceptable limits, but, unlike many other fluoroalkyl(aqua) complexes we have prepared,[4,5,39] we cannot provide unambiguous IR or NMR data for the presence of a coordinated water ligand. The overall stereochemistry at Pt is retained in **11**, as evidenced by diastereotopic α- and β-CF_2 groups and inequivalent Pt-Me groups in the NMR spectra. In addition, **11** reacts with NaCl to produce a corresponding chloro analogue **12** that is isostructural with **6**, as indicated by ^{1}H and ^{19}F NMR spectroscopy. The fact that the transformation of **6a** → **11** → **12** can be accomplished with retention of stereochemistry indicates that the cation **8** is probably configurationally stable.

Based on this accumulation of circumstantial evidence, it seems that either the initial oxidative addition of perfluoro-*n*-propyl iodide to give **6a** occurs via an overall concerted *cis* addition or the initially formed cation **7** rearranges to **8** quickly compared to the rate at which iodide reacts at platinum. However, analogous cations containing basal methyl and axial perdeuteriomethyl groups scramble via an analogous rearrangement on a time scale reported to be slow compared to the rate of trapping of the cation by iodide,[40] so the notion of a concerted addition in our case may not be far fetched.

Reaction of complex **9a** with 1 equiv of I_2 affords the Pt(IV) product (TMEDA)Pt(*n*-C_3F_7)(CH_3)I_2, **13**, as a deep red crystalline solid (Scheme 2). Proton NMR spectroscopy shows only two environments for the NMe groups, indicating that the two iodide ligands are either both *trans* or both *cis*; the *trans* configuration is confirmed by X-ray crystallography, and an ORTEP is shown in Figure 5.

In contrast to **6a**, with a labile iodide *trans* to a CH_3 ligand, the iodide in complex **13** is far less labile, and reductive elimination of CH_3I in $CDCl_3$ solution is very slow, forming an approximately 1:1 mixture with **14**

(39) Hughes, R. P.; Lindner, D. C.; Smith, J. M.; Zhang, D.; Incarvito, C. D.; Lam, K.-C.; Liable-Sands, L. M.; Sommer, R. D.; Rheingold, A. L. *J. Chem. Soc., Dalton Trans.* **2001**, in press.

(40) Jenkins, H. A.; Yap, G. P. A.; Puddephatt, R. J. *Organometallics* **1997**, *16*, 1946−1955.

Scheme 3

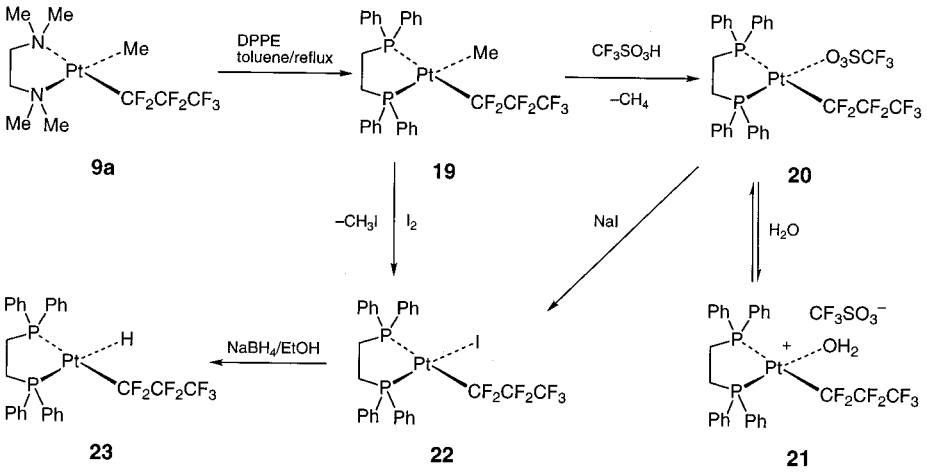

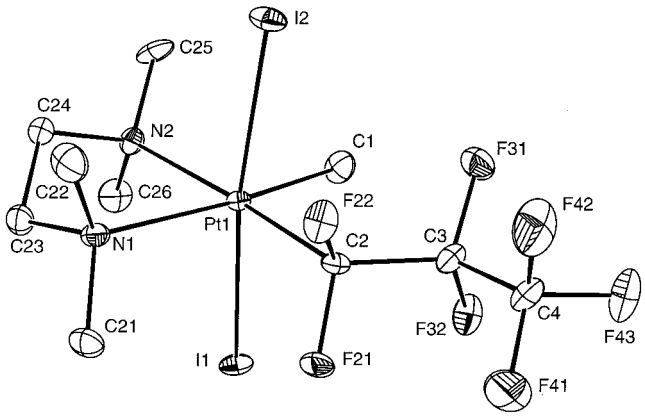

Figure 5. ORTEP diagram of the non-hydrogen atoms of **13**, showing atom-labeling scheme. Thermal ellipsoids are shown at the 30% level.

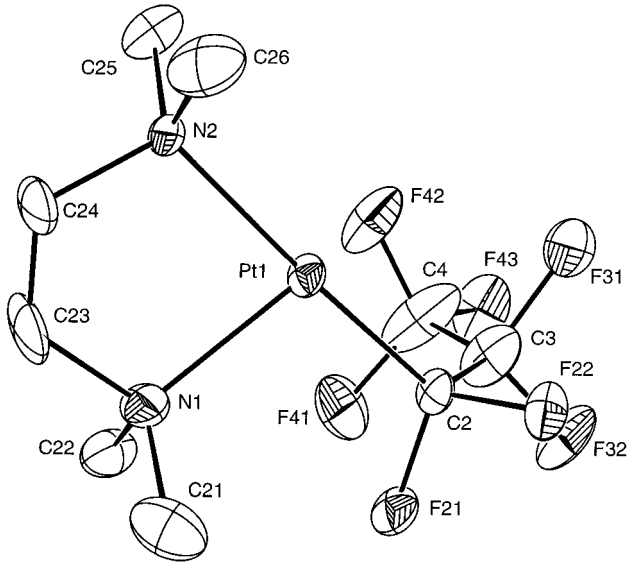

Figure 6. ORTEP diagram of the non-hydrogen atoms of **18**, showing atom-labeling scheme. Thermal ellipsoids are shown at the 30% level.

after 3 weeks. Addition of excess NaI in EtOH only slightly accelerates the conversion of **13** to **14**, which is complete after 4 weeks. However, reaction of **13** with $AgBF_4$ followed by addition of NaI cleanly produces the Pt(II) complex **14** as a yellow solid. We assume that this reaction proceeds by initial removal of one of the iodide ligands by Ag^+ to form cation **15**, which, on addition of iodide nucleophile, rapidly eliminates CH_3I via attack at CH_3 to form **14**. We must also assume that cation **15** can rearrange to isomer **16** with an axial methyl in order for such a nucleophilic attack to produce square planar **14**. This cation rearrangement is analogous to that proposed for the conversion of **7** to **8** during formation of **6a** (vide supra). The observation that elimination of CH_3I from **16** does not occur without added nucleophile (I^-) suggests that it is direct nucleophilic attack on the CH_3 group of **16** that is responsible for reductive elimination.[25,41] Analogous nucleophilic attack by water on the CH_3 ligand of a cationic Pt(IV) intermediate has been identified as a key step in the reductive elimination of methanol.[42]

Reaction of complex **9a** with CF_3SO_3H (HOT_f) in moist CH_2Cl_2 produces the cationic Pt(II) complex **17**, which forms an equilibrium in acetone-d_6 solution, after a few hours, with a second compound, presumably [(TMEDA)-$Pt(C_3F_7)\{(CD_3)_2CO\}]OT_f$. Addition of excess H_2O reforms **17**. This cationic complex reacts with iodide to afford the iodo(fluoropropyl) complex **14**. Complex **14** reacts with $NaBH_4$ in EtOH solution to produce the hydride complex **18**, which has a metal hydride resonance at δ −20.96 ppm and a Pt−H stretch in the IR spectrum at 2197 cm^{-1}. This compound has also been characterized crystallographically, and an ORTEP is shown in Figure 6.

Perfluoroalkyl Pt(II) Complexes with Diphosphine Ligands. The TMEDA ligand in these Pt(II) complexes can be displaced by chelating diphosphine ligands, as shown in Scheme 3. Complex **9a** reacts with 1,2-bis(diphenylphosphino)ethane (DPPE) in refluxing toluene to afford the corresponding diphosphine analogue **19**; the structure of **19** was confirmed crystallographically, and an ORTEP is shown in Figure 7. Treatment of **19** with HOT_f affords a white solid triflate complex **20**, presumably with liberation of methane; no elimination of fluoroalkane was observed. The structure of **20** was also confirmed crystallographically, and an ORTEP is presented in Figure 8. In moist CD_2Cl_2

(41) Crumpton, D. M.; Goldberg, K. I. *J. Am. Chem. Soc.* **2000**, *122*, 962−963.
(42) Luinstra, G. A.; Labinger, J. A.; Bercaw, J. E. *J. Am. Chem. Soc.* **1993**, *115*, 3004−3005.

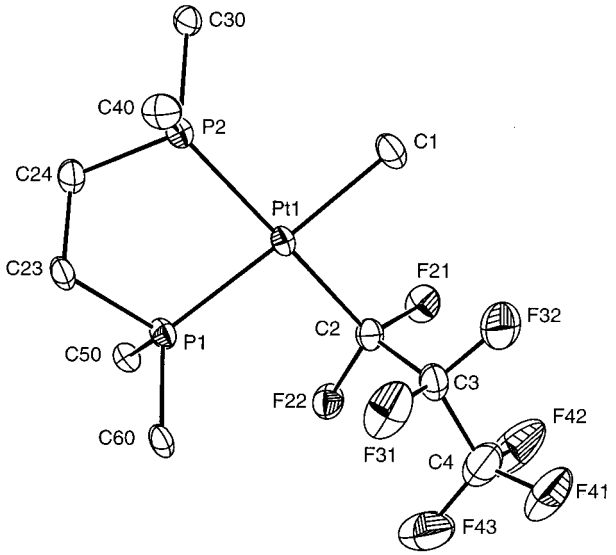

Figure 7. ORTEP diagram of the non-hydrogen atoms of **19**, showing atom-labeling scheme. Only the ipso-carbons of each phenyl ring are shown for clarity. Thermal ellipsoids are shown at the 30% level.

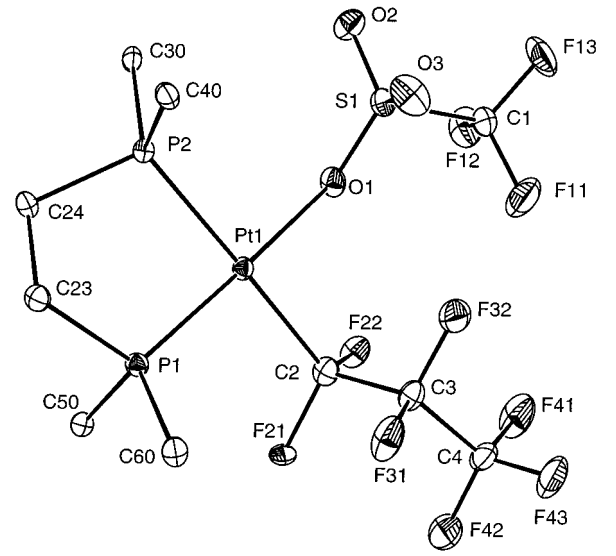

Figure 8. ORTEP diagram of the non-hydrogen atoms of **20**, showing atom-labeling scheme. Only the ipso-carbons of each phenyl ring are shown for clarity. Thermal ellipsoids are shown at the 30% level.

solution at room temperature the ^{19}F NMR spectrum of this complex shows two sets of broad resonances for the triflate and fluoroalkyl ligands in an approximately 1:1 ratio. We attribute this behavior to the presence of an equilibrium between **20** and a water complex **21**, analogous to the TMEDA analogue **17**. Cooling the sample or addition of water to the NMR sample at room temperature shifts the equilibrium toward **21**. However, unlike the TMEDA analogue **17**, it is the coordinated triflate complex **20** that crystallizes, even from moist solvents, perhaps illustrating the difference in affinity for water between the harder (TMEDA)Pt center compared to the softer (DPPE)Pt analogue.

In contrast to the reaction of the TMEDA analogue **9a** with I_2, to afford the Pt(IV) complex **13**, reaction of the DPPE complex **19** with I_2 affords only the Pt(II) complex **22**, which can also be prepared cleanly by

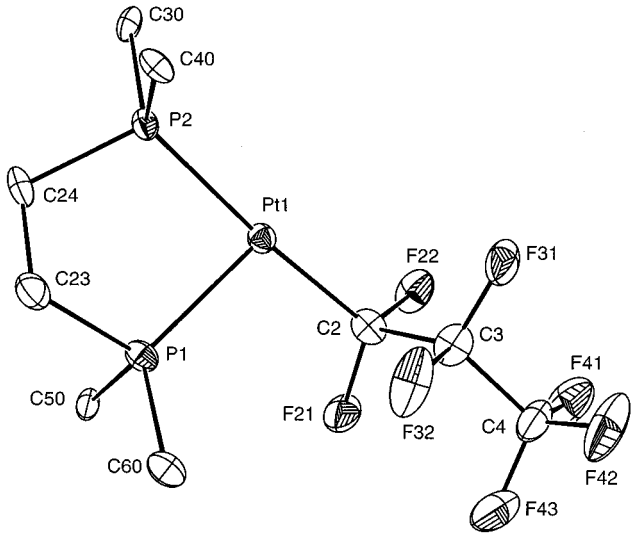

Figure 9. ORTEP diagram of the non-hydrogen atoms of one of the two independent molecules of **23**, showing atom-labeling scheme. Only the ipso-carbons of each phenyl ring are shown for clarity. Thermal ellipsoids are shown at the 30% level.

reaction of the triflate complex **20** with sodium iodide. Clearly, elimination of CH_3I from a Pt(IV) intermediate is more facile with DPPE as a ligand than with TMEDA. This may be a steric effect, as we observe that analogous eliminations from 1,2-(dimethylphosphino)ethane Pt(IV) complexes are actually more difficult than from TMEDA analogues.[43] Treatment of **22** with $NaBH_4$ in ethanol affords the hydride complex **23** in high yield. A similar complex, (DPPE)Pt(CF_3)H, has been prepared in a similar manner.[44−47] The proton and fluorine NMR spectra of **23** show complex coupling patterns. The hydride couples with the platinum (J = 1209 Hz), the *trans*-phosphorus (J = 189 Hz), the *cis*-phosphorus (J = 15 Hz), the α-CF_2 (J = 7.5 Hz), and the β-CF_2 (J = 6.5 Hz). The α-CF_2 couples with the platinum (J = 379 Hz), the *trans*-phosphorus (J = 32.6 Hz), the *cis*-phosphorus (J = 31.7 Hz), the CF_3 (J = 10 Hz), and the hydride (J = 7.5 Hz). In fluoroalkyl groups $^3J_{FF}$ is often close to zero[48] and is not observed in our compounds. Interestingly, the β-CF_2 couples with the platinum (J = 150 Hz), the hydride (J = 6.5 Hz), and only to the *cis*-phosphorus (J = 7.3 Hz). This particular phosphorus, which is also *trans* to the hydride ligand, can be unambiguously assigned by using non-proton-decoupled ^{31}P NMR; it has the large coupling to the hydride, as expected. The structure of **23** was confirmed by X-ray crystallography. The compound crystallizes with two independent molecules in the asymmetric unit; an ORTEP of one molecule is shown in Figure 9.

It is noteworthy that none of the water complexes **11**, **17**, or **21** show any evidence of hydrolysis reactions of

(43) Hughes, R. P.; Sweetser, J. T.; Tawa, M. D.; Williamson, A. Unpublished observations.
(44) Michelin, R. A.; Ros, R.; Guadalupi, G.; Bombieri, G.; Benetollo, F.; Chapuis, G. *Inorg. Chem.* **1989**, *28*, 840−846.
(45) Michelin, R. A.; Belluco, U.; Ros, R. *Inorg. Chim. Acta* **1977**, *24*, L33−L34.
(46) Michelin, R. A.; Facchin, G.; Ros, R. *J. Organomet. Chem.* **1985**, *279*, C25−C28.
(47) Del Pra, A.; Zanotti, G.; Bardi, R.; Belluco, U.; Michelin, R. A. *Cryst. Struct. Commun.* **1979**, *8*, 729−736.
(48) Emsley, J. W.; Phillips, L.; Wray, V. *Fluorine Coupling Constants*; Pergamon: Oxford, 1977.

Table 2. Selected Bond Lengths (Å) and Angles (deg) for the Coordination Spheres of Pd(II)− and Pt(II)−Fluoroalkyl Complexes

	3a[35]	**3b**[35]	**9a**	**9b**	**18**	**19**	**20**	**23**
Pt−X(1)	2.106(10), 2.078(10	2.052(5)	2.148(18)[a]	2.060(5)[a]	*b*	2.108(7)[a]	2.142(4)[c]	*b*
Pt−C(2)	1.996(9), 1.970(11)	1.990(5)	2.01(2)	1.995(4)	1.996(10)	2.067(7)	2.087(6)	2.049(13), 2.074(14)
Pt−E(1)	2.222(8), 2.228(8)	2.235(4)	2.14(2)[d]	2.205(4)[d]	2.155(10)[d]	2.2984(19)[e]	2.2062(14)[e]	2.331(3),[e] 2.313(3)[e]
Pt−E(2)	2.162(9), 2.139(9)	2.167(4)	2.172(19)[d]	2.161(3)[d]	2.123(8)[d]	2.2832(19)[e]	2.3094(14)[e]	2.264(3),[e] 2.259(3)[e]
X(1)−Pt−C(2)	86.8(4), 87.2(4)	87.7(2)	88.3(9)	89.02(18)[a]	*b*	89.0(3)[a]	86.0(2)[a]	*b*
E(1)−Pt−E(2)	82.1(3), 82.6(3)	82.39(18)	81.7(8)[d]	82.72(14)[d]	82.4(3)[d]	84.91(7)[e]	85.34(5)[e]	85.47(12),[e] 85.57(11)[e]
X(1)−Pt−E(2)	92.6(4), 91.7(4)	92.0(2)	92.3(8)	91.09(17)	*b*	92.3(2)	94.85(11)	*b*
C(2)−Pt−E(1)	98.6(3), 98.6(4)	97.97(19)	97.7(9)	97.21(15)	100.2(4)	93.8(2)	93.8(2)	99.3(4), 98.6(4)

[a] X = CH_3. [b] X = H. [c] X = O. [d] E = N. [e] E = P.

the α-CF_2 groups, as has been observed in analogous fluoroalkyl(aqua) cations of Rh(III).[4] Furthermore, treatment of the water complexes **11**, **17**, or **21** or the triflate complex **20** with H_2 results in no reaction, affording no evidence of any hydrogenolysis of the α-CF_2 bonds, as has been observed in analogous compounds of Ir(III).[5] It seems clear that fluorines on a carbon α to Pt(II) or Pt(IV) are much less labile than those α to Rh(III) or Ir(III).

Dynamic Behavior of the TMEDA Rings. We have shown previously that the ^{19}F NMR spectra of palladium complexes **3** and **4** are temperature dependent, due to a slowing of the ring pucker inversion of the TMEDA ring at low temperatures, a process with $\Delta G^{\ddagger} = 11-13$ kcal mol^{-1}.[35] In a puckered ring ground state there is a stereocenter at the metal, and the α-CF_2 and β-CF_2 groups contain diastereotopic fluorines. At low temperatures each pair of diastereotopic fluorines appears as a well-separated, and strongly coupled, AX spin system, each of which coalesces as the temperature is raised. In iodo complex **4** the chemical shift difference between the α-CF_2 fluorines is so large (∼35 ppm at 470 MHz) that their coalescence temperature is close to ambient, and at room temperature the α-CF_2 resonance is invisible.

Like its palladium analogue **4**,[35] the room-temperature ^{19}F NMR spectrum of **14** in toluene-d_8 shows only a CF_3 triplet and a broad β-CF_2 singlet. As pointed out earlier, in fluoroalkyl groups $^3J_{FF}$ is often close to zero[48] and is unobserved in our compounds. Consequently, the CF_3 triplet arises from a ^4J coupling to the α-CF_2 rather than to the β-CF_2 fluorines, but the α-CF_2 resonance itself is not observed. On progressive cooling, the β-CF_2 resonance separates into two doublets corresponding to two diastereotopic fluorines, and two broad humps begin to appear, corresponding to two diastereotopic α-CF_2 fluorines. At −60 °C these become two sharp doublets, well separated by 29.8 ppm (at 470 MHz), but with platinum satellites still too broad to observe, probably due to chemical shift anisotropy effects that have been well documented in other compounds.[49−55] When the sample of **14** is heated to 90 °C, the β-CF_2 fluorines are observed as a sharp singlet with platinum satellites and the α-CF_2 has also begun to sharpen to a singlet.

Similar behavior is observed for **9a**, in which the α-CF_2 resonance at room temperature is broad in CD_2Cl_2 solution. At −70 °C both the α- and β-CF_2 resonances separate into four sharp doublet resonances, with a large coupling between the two individual β-CF_2 fluorines ($^2J_{FF}$ = 284 Hz) and between the two individual α-CF_2 fluorines ($^2J_{FF}$ = 272 Hz). While the platinum satellites for the β-CF_2 fluorines are broad and appear as narrow shoulders, those for the α-CF_2 fluorines are only slightly broadened and are dramatically different for each fluorine atom ($^2J_{F1Pt}$ = 535 Hz, $^2J_{F2Pt}$ = 285 Hz). The F−Pt coupling constant for the α-CF_2 group at room temperature is the approximate mean of these two values ($^2J_{FPt}$ = 429 Hz). The separation between the two α-CF_2 resonances at −70 °C is 5.5 ppm. The ^1H NMR spectra of **9a** at room temperature and at −70 °C both show only two environments for the NMe groups, indicating that the chemical shift difference is small and decoalescence has not yet occurred. However, the −70 °C spectrum shows four separate environments for the hydrogens of the CH_2CH_2 backbone and very broad Pt-satellites.

The room-temperature ^{19}F NMR spectrum of the hydrido analogue **18** in CD_2Cl_2 is sharp. However, on cooling to −20 °C, the resonances corresponding to the α- and β-CF_2 fluorines begin to broaden, and at −75 °C the α-CF_2 fluorines appear as two doublets ($^2J_{FF}$ = 276 Hz) with different platinum couplings ($^2J_{F1Pt}$ = 384 Hz, $^2J_{F2Pt}$ = 328 Hz), though not as dramatically different as those in **9a**. In contrast to **14** and **9a**, the diastereotopic α-CF_2 resonances are only separated by 1.4 ppm.

The Pt(IV) complex **13** has the same symmetry as **14**, and its ^{19}F NMR spectrum at room temperature shows equivalent fluorines within each CF_2 group. On cooling to −20 °C, the resonances corresponding to the α- and β-CF_2 groups start to become broad and at −70 °C separate into four broad humps. The TMEDA ring puckering process in this platinum(IV) complex appears to be more facile than that in the Pt(II) analogues.

Structural Comparisons. Details of the crystal structure determinations of all compounds determined here are presented in Table 1. Selected bond lengths and angles for the square planar Pt(II) compounds are presented in Table 2, along with comparison data for **3a** and **3b**. Analogous values for octahedral Pt(IV) compounds appear in Table 3. To allow for easy comparison, in each series a common numbering system is used, with atom X(1) [X = CH_3, H, O] always *trans* to E(1) (E = N, P), and atom C(2) (the α-carbon of the fluorinated ligand) always *trans* to E(2). In the Pt(IV)

(49) Skvortsov, A. N. *Russ. J. Gen. Chem.* **2000**, *70*, 1023−1027.
(50) Ghosh, P.; Desrosiers, P. J.; Parkin, G. *J. Am. Chem. Soc.* **1998**, *120*, 10416−10422.
(51) Gay, I. D.; Young, G. B. *Organometallics* **1996**, *15*, 2264−2269.
(52) Lindner, E.; Fawzi, R.; Mayer, H. A.; Eichele, K.; Hiller, W. *Organometallics* **1992**, *11*, 1033−1043.
(53) Ismail, I. M.; Kerrison, S. J. S.; Sadler, P. J. *Polyhedron* **1982**, *1*, 57−59.
(54) Doddrell, D. M.; Barron, P. F.; Clegg, D. E.; Bowie, C. *J. Chem. Soc., Chem. Commun.* **1982**, 575−576.
(55) Lallemand, J. Y.; Soulie, J.; Chottard, J. C. *J. Chem. Soc., Chem. Commun.* **1980**, 436−438.

Table 3. Selected Bond Lengths (Å) and Angles (deg) for the Coordination Sphere of Pt(IV)−Fluoroalkyl Complexes

	6a	10	13
Pt−C(1)	2.064(9)	2.092(14)	2.098(10)
Pt−C(2)	2.050(6)		2.083(9)
Pt−C(1A)	2.077(6)		
Pt−N(1)	2.275(7)	2.282(11)	2.312(7)
Pt−N(2)	2.226(5)		2.262(7)
Pt−I(1)	2.8037(5)	2.6731(10)	2.6936(6)
Pt−I(2)			2.6916(6)
C(1)−Pt−C(2)	95.4(3)	91.4(10)	96.6(3)
N(1)−Pt−N(2)	82.5(2)	82.8(5)	82.3(2)
C(1)−Pt−N(2)	89.5(3)	92.9(6)	88.5(3)
C(2)−Pt−N(1)	92.7(2)		92.6(3)
C(1A)−Pt(1)−N(1)	92.2(3)		
C(2)−Pt(1)−I(1)	89.81(17)		88.5(2)
C(1)−Pt(1)−I(1)	85.9(2)	85.9(4)	84.6(2)
N(2)−Pt(1)−I(1)	93.77(13)	93.2(3)	92.37(17)
N(1)−Pt(1)−I(1)	93.15(15)	96.4(3)	93.97(12)

complexes the "equatorial plane" is used to mean the plane corresponding to N(1) and N(2) and the two atoms *trans* to them. Two sets of data are presented for **23**, corresponding to the two independent molecules in the asymmetric unit.

We have presented elsewhere a discussion of the structural *trans* influences[56] of perfluoroalkyl and methyl ligands in (TMEDA)Pd complexes **3**.[35] The structure of **9a** is of sufficiently poor quality to preclude meaningful comparisons, but its perfluoroethyl analogue **9b** illustrates the expected shorter bond to the fluoroalkylated carbon than to the CH_3 ligand, and the lower *trans* influence of fluoroalkyl compared to methyl. Comparison with the structure of Pd analogue **3b** illustrates that the compounds are virtually identical in terms of bond lengths to the metal center. Comparison of **9b** with the hydrido complex **18** is also interesting; the Pt−fluoroalkyl distance remains unchanged, but both Pt−N distances are significantly shorter in **18** than in **9b**. The shortening of the Pt−N(2) distance *trans* to R_F may reflect the reduced steric demand of the *cis* ligand H relative to CH_3, while the corresponding shortening of the Pt−N(1) distance may reflect a weaker *trans* influence of H relative to CH_3 in these systems. These differences also illustrate the difficulty of isolating *cis* steric influences from *trans* electronic influences in comparing bond distances and emphasize the dangers of overinterpretation of bond length data.

Some useful comparisons can be made with the series of DPPE analogues. Comparison of **9b** with **19** shows that both Pt−C bonds are significantly longer in the diphosphine complex, perhaps reflecting the greater *trans* influence of P compared to N, but perhaps also reflecting a difference in *cis* steric influences of the two chelating ligands. The Pt−fluoroalkyl distance is still shorter than the Pt−CH_3 distance, and the fluoroalkyl *trans* influence is still weaker than the corresponding influence of CH_3. Therefore, the order of *trans* influences of fluoroalkyl versus CH_3 holds for diamine ligands, which cannot be π-acceptors, and diphosphine ligands, which can. This supports the proposal[57] that π-acceptor properties of ligands are relatively unimportant in determining *trans* influences. However it is also interesting that, in a comparison of **19** and **23**, the Pt−P(1) distance *trans* to H in **23** is significantly longer than that *trans* to CH_3 in **19**, exactly the opposite of the observation in the TMEDA analogues discussed above. The Pt−P(2) bond *cis* to H in **23** is shorter than that *cis* to CH_3 in **19**, once again illustrating that *cis* steric influences may be more important than any *trans* influences in determining bond distances. The Pt−P(1) distance in triflate complex **20** illustrates that triflate has a weaker *trans* influence than CH_3 or H, but the lengthening of the Pt−P(2) distance in **20** compared to those in **19** and **23** is most likely a reflection of the larger steric demand of triflate.

The series of octahedral Pt(IV) complexes **6a**, **10**, and **13** (Table 3) provide analogous comparisons within the series and also with their square planar Pt(II) analogues (Table 2). In each of **6a** and **13** the Pt distances to fluoroalkyl and CH_3 are no longer significantly different, but the bonds to the N still reflect the lower *trans* influence of fluoroalkyl compared to CH_3 in each compound. All bonds in the "equatorial" plane of **13** are longer than those in **6a**, probably reflecting the steric effects of two "axial" iodides in the former compound compared to a single iodide and a methyl in the latter. The Pt−CH_3 distance in **10** is identical to that in **13** and longer than that in **6a**, probably for the same reason. Once again it is difficult to separate steric effects from any electronic effects on bond distances.

Experimental Section

General Considerations. Unless otherwise noted, all reactions were performed in oven-dried glassware, using standard Schlenk techniques, under an atmosphere of nitrogen, which had been deoxygenated over BASF catalyst and dried using Aquasorb, or using drybox techniques. THF, diethyl ether, hexanes, and CH_2Cl_2 were dried and degassed over alumina columns under N_2.[58] ^{1}H NMR (300 MHz) and ^{19}F (282 MHz) were recorded on a Varian UNITY plus 300 system in the solvent indicated. Variable-temperature ^{1}H (500 MHz) and ^{19}F (470 MHz) NMR spectra were recorded on a Varian UNITY plus 500 system in the solvent indicated. ^{1}HNMR chemical shifts were referenced to TMS using the protio impurity in the solvent peak, and ^{19}F chemical shifts were referenced to $CFCl_3$. Microanalyses were performed by Schwarzkopf Microanalytical Laboratory (Woodside, NY).

Perfluoroalkyl iodides were purchased from Aldrich, treated with $Na_2S_2O_3$ to remove residual I_2, and vacuum distilled before use. (TMEDA)Pt$(CH_3)_2$ was prepared according to a literature procedure.[59]

(TMEDA)Pt(*n*-C_3F_7)$(CH_3)_2$I (6a). To a stirring suspension of (TMEDA)Pt$(CH_3)_2$ (0.564 g, 1.65 mmol) in hexanes (20 mL) was added *n*-C_3F_7I (0.40 mL, 2.77 mmol). The solid rapidly dissolved to form a yellow solution, followed by slow precipitation of a white solid. The mixture was stirred for 16 h and then filtered. The solid residue was washed with hexanes and air-dried. Yield: 0.854 g, 81%. Anal. Calcd for $C_{11}H_{22}F_7IN_2Pt$: C, 20.73; H, 3.48; N, 4.39. Found: C, 20.80; H, 3.47; N, 4.34. ^{1}H NMR ($CDCl_3$, 300 MHz, 23 °C): δ 1.42 (m, 3H, $^2J_{HPt} = 64.2$ Hz, PtMe), 1.74 (t, $^4J_{HF} = 2.0$ Hz, 3H, $^2J_{HPt} = 69.3$ Hz, PtMe), 2.42 (s, 3H, $^3J_{HPt} = 18.6$ Hz, NMe), 2.61 (s, 3H, $^3J_{HPt} = 12.9$ Hz, NMe), 2.61−3.90 (m, 4H, CH_2), 3.30 (s, 3H, $^3J_{HPt} = 15.0$

(56) Appleton, T. G.; Clark, H. C.; Manzer, L. E. *Coord. Chem. Rev.* **1973**, *10*, 335−422.
(57) Landis, C. R.; Firman, T. K.; Root, D. M.; Cleveland, T. *J. Am. Chem. Soc.* **1998**, *120*, 1842−1854.
(58) Pangborn, A. B.; Giardello, M. A.; Grubbs, R. H.; Rosen, R. K.; Timmers, F. J. *Organometallics* **1996**, *15*, 1518−1520.
(59) Yang, D. S.; Bancroft, G. M.; Dignard-Bailey, L.; Puddephatt, R. J.; Tse, J. S. *Inorg. Chem.* **1990**, *29*, 2487−2495.

Hz, NMe), 3.35 (s, 3H, $^3J_{HPt}$ = 9.3 Hz, NMe). ^{19}F NMR ($CDCl_3$, 282.2 MHz, 23 °C): δ −119.9 (d,$^2J_{FF}$ = 284 Hz, β-CF), −117.2 (d, $^2J_{FF}$ = 284 Hz, β-CF), −81.1 (dm, $^2J_{FF}$ = 257 Hz, $^2J_{FPt}$ = 300 Hz, α-CF), −79.6 (t, $^4J_{FF}$ = 13 Hz, $^4J_{FPt}$ = 20 Hz, CF_3), −64.6 (dm, $^2J_{FF}$ = 257 Hz, $^2J_{FPt}$ = 251 Hz, α-CF). Crystals for the structure determination were obtained from CH_2Cl_2−hexane at −20 °C as yellow blocks.

(TMEDA)Pt(C_2F_5)(CH_3)$_2$I (6b). To a suspension of (TMEDA)Pt(CH_3)$_2$ (0.100 g, 0.293 mmol) in hexanes (20 mL) was added CF_3CF_2I (0.2 g, 0.82 mmol). The mixture was stirred overnight at room temperature in the absence of light. The resulting white suspension was filtered, and the residue was washed with hexanes (3 × 5 mL). The white solid was dissolved in CH_2Cl_2 (5 mL) and filtered through Celite. The colorless filtrate was collected, and the product was precipitated upon addition of hexanes (20 mL). The white solid was dried in vacuo to give the product, 0.143 g, 83%. Anal. Calcd for $C_{10}H_{22}F_5IN_2Pt$: C 20.45, H 3.78. Found: C 20.60, H 3.64. ^{1}H NMR (C_6D_6, 300 MHz, 23 °C): δ 1.09 (d, $^2J_{HPt}$ = 64 Hz, $^4J_{HF}$ = 2 Hz, 3H, $PtCH_3$), 1.34−1.55 (m, 2H, CH_2), 1.39 (s, $^3J_{HPt}$ = 18 Hz, 3H, NCH_3), 1.82 (s, $^2J_{HPt}$ = 70 Hz, 3H, $PtCH_3$), 1.87 (s, $^3J_{HPt}$ = 13 Hz, 3H, NCH_3), 1.97−2.18 (m, 2H, CH_2), 2.74 (s, $^3J_{HPt}$ = 15 Hz, 3H, NCH_3), 3.01 (s, $^3J_{HPt}$ = 10 Hz, 3H, NCH_3). ^{19}F NMR (C_6D_6, 282.2 MHz, 23 °C): δ −83.7 (d, $^2J_{FPt}$ = 331 Hz, $^2J_{FF}$ = 252 Hz, CF), −77.3 (s, CF_3), −70.2 (d, $^2J_{FF}$ = 252 Hz, $^2J_{FPt}$ = 245 Hz, CF).

[(TMEDA)Pt(*n*-C_3F_7)(CH_3)$_2$(OH_2)]BF_4 (11). On addition of toluene (15 mL) to a mixture of (TMEDA)Pt(*n*-C_3F_7)(CH_3)$_2$I (0.101 g, 0.158 mmol) and $AgBF_4$ (0.045 g, 0.23 mmol) a pale yellow suspension was formed. The mixture was stirred for 16 h and then filtered through Celite, which was washed further with CH_2Cl_2. The solvent was removed in vacuo from the resultant filtrate to give a white solid, which was washed with $CHCl_3$. Yield: 0.088 g, 90%. Anal. Calcd for $C_{11}H_{24}BF_{11}N_2OPt$: C, 21.48; H, 3.93; N, 4.55. Found: C, 21.63; H, 4.36; N, 4.42. ^{1}H NMR (CD_2Cl_2, 300 MHz, 23 °C): δ 1.34 (s, 3H, $^2J_{HPt}$ = 76 Hz, PtMe), 1.34 (s, 3H, $^2J_{HPt}$ = 66 Hz, PtMe), 2.49 (s, 3H, $^3J_{HPt}$ = 22.5 Hz, NMe), 2.58 (s, 3H, $^3J_{HPt}$ = 14.4 Hz, NMe), 2.66−3.22 (m, 10H, NMe and CH_2). ^{19}F NMR (CD_2Cl_2, 282.2 MHz, 23 °C): δ −149.9 (s, BF_4), −121.3 (dd, $^2J_{FF}$ = 289 Hz, $^3J_{FF}$ = 14 Hz, β-CF), −119.9 (d, $^2J_{FF}$ = 289 Hz, β-CF), −91.8 (ddq, $^2J_{FF}$ = 272 Hz, $^3J_{FF}$ = 14 Hz, $^4J_{FF}$ = 13 Hz, $^2J_{FPt}$ = 389 Hz, α-CF), −89.3 (dm, $^2J_{FF}$ = 272 Hz, $^2J_{FPt}$ = 220 Hz, α-CF), −80.1 (t, $^4J_{FF}$ = 13 Hz, $^4J_{FPt}$ = 16 Hz, CF_3).

(TMEDA)Pt(*n*-C_3F_7)(CH_3)$_2$Cl (12). Addition of CH_2Cl_2 (15 mL) to a mixture of (TMEDA)Pt(*n*-C_3F_7)(CH_3)$_2$I (0.200 g, 0.319 mmol) and $AgBF_4$ (0.080 g, 0.411 mmol) gave a yellow precipitate of AgI. The mixture was stirred for 1 h, and then a solution of NaCl (0.3 g, excess) in EtOH/H_2O was added. After stirring for 30 min the volatiles were removed in vacuo and the solid residue was extracted into CH_2Cl_2 and then filtered through Celite. Removal of solvent in vacuo gave a white solid. Yield: 0.165 g, 96%. Anal. Calcd for $C_{11}H_{22}ClF_7N_2Pt$: C, 24.20; H, 4.06; N, 5.13. Found: C, 23.98; H, 4.13; N, 5.07. ^{1}H NMR ($CDCl_3$, 300 MHz, 23 °C): δ 1.12 (d, 3H, $^4J_{HF}$ = 2.7 Hz, $^2J_{HPt}$ = 69 Hz, PtMe), 1.36 (s, 3H, $^2J_{HPt}$ = 69 Hz, PtMe), 2.43 (s, 3H, $^3J_{HPt}$ = 19.5 Hz, NMe), 2.54 (s, 3H, $^3J_{HPt}$ = 12.6 Hz, NMe), 2.84 (s, 3H, $^3J_{HPt}$ = 13.5 Hz, NMe), 2.99 (s, 3H, $^3J_{HPt}$ = 8.4 Hz, NMe), 2.38−3.14 (m, 4H, CH_2). ^{19}F NMR ($CDCl_3$, 282.2 MHz, 23 °C): δ −121.1 (dd, $^2J_{FF}$ = 289 Hz, $^3J_{FF}$ = 13 Hz, β-CF), −119.0 (ddd, $^2J_{FF}$ = 289 Hz, $^3J_{FF}$ = 12 Hz, $^3J_{FF}$ = 8 Hz, β-CF), −86.6 (ddq, $^2J_{FF}$ = 270 Hz, $^3J_{FF}$ = 12 Hz, $^4J_{FF}$ = 13.5 Hz, $^2J_{FPt}$ = 388 Hz, α-CF), −83.2 (dddq, $^2J_{FF}$ = 270 Hz, $^3J_{FF}$ = 13 Hz, $^3J_{FF}$ = 8 Hz, $^4J_{FF}$ = 15 Hz, $^2J_{FPt}$ = 246 Hz, α-CF), −79.7 (dd, $^4J_{FF}$ = 13.5 Hz, $^4J_{FF}$ = 15 Hz, $^4J_{FPt}$ = 19 Hz, CF_3).

(TMEDA)Pt(*n*-C_3F_7)(CH_3) (9a). To a solution of (TMEDA)-Pt(*n*-C_3F_7)(CH_3)$_2$I (0.105 g, 0.165 mmol) in moist acetone (15 mL) was added Et_3N (2 mL, excess) and the pale yellow solution stirred for 16 h. The solvent was removed in vacuo and the resultant solid treated with Et_2O. The white precipitate of (Et_3NMe)I was removed by filtration and the resultant filtrate reduced in vacuo to afford a yellow solid. Yield: 0.082 g, 99%. Anal. Calcd for $C_{10}H_{19}F_7N_2Pt$: C, 24.25; H, 3.84; N, 5.65. Found: C, 24.22; H, 3.84; N, 5.65. ^{1}H NMR ($CDCl_3$, 300 MHz, 23 °C): δ 0.50 (tt, $^4J_{HF}$ = $^5J_{HF}$ = 1.5 Hz, 3H, $^2J_{HPt}$ = 86.1 Hz, PtMe), 2.64 (s, 6H, $^3J_{HPt}$ = 26.1 Hz, NMe), 2.54−2.73 (m, 4H, CH_2), 2.77 (s, 6H, $^3J_{HPt}$ = 18 Hz, NMe). ^{1}H NMR (CD_2Cl_2, 500 MHz, −70 °C): δ 0.25 (s, 3H, PtMe), 2.24 (br d, J_{HH} = 11 Hz, 1H, CH_2), 2.41 (br d, J_{HH} = 11 Hz, 1H, CH_2), 2.56 (s, 6H, NMe), 2.66 (s, 6H, NMe), 2.83 (br t, J_{HH} = 13 Hz, 1H, CH_2), 2.92 (br t, J_{HH} = 13 Hz, 1H, CH_2). ^{19}F NMR ($CDCl_3$, 300 MHz, 23 °C): δ −118.2 (s, $^3J_{FPt}$ = 118 Hz, β-CF_2), −90.3 (br s, $^2J_{FPt}$ = 429 Hz, α-CF_2), −79.7 (t, $^4J_{FF}$ = 11 Hz, $^4J_{FPt}$ = 36 Hz, CF_3). ^{19}F NMR (CD_2Cl_2, 470.4 MHz, −70 °C): δ −117.9 (d, $^2J_{FF}$ = 284 Hz, β-CF), −114.8 (d, $^2J_{FF}$ = 284 Hz, β-CF), −92.1 (d, $^2J_{FF}$ = 272 Hz, $^2J_{FPt}$ = 285 Hz, α-CF), −86.6 (d, $^2J_{FF}$ = 272 Hz, $^2J_{FPt}$ = 535 Hz, α-CF), −77.8 (t, $^4J_{FF}$ = 10.5 Hz, CF_3).

(TMEDA)Pt(C_2F_5)(CH_3) (9b). To a solution of (TMEDA)-Pt(C_2F_5)(CH_3)$_2$I (0.101 g, 0.172 mmol) in acetone (20 mL) was added Et_3N (2.0 mL, 14 mmol). The colorless solution was stirred overnight under reflux. The solution was cooled to room temperature, and the volatiles were removed in vacuo to yield a white solid. The solid was extracted into Et_2O and filtered through Celite. The filtrate was collected, and the volatiles were removed in vacuo to yield the product as a white solid (0.070 g, 91%). Anal. Calcd for $C_9H_{19}F_5N_2Pt$: C 24.27, H 4.30. Found: C 24.17, H 4.20. ^{1}H NMR (C_6D_6, 300 MHz, 23 °C): δ 0.97 (tq, $^2J_{HPt}$ = 88 Hz, $^4J_{HF}$ = 1 Hz, $^5J_{HF}$ = 1 Hz, 3H, $PtCH_3$), 1.34−1.44 (m, 4H, CH_2CH_2), 1.80 (s, $^3J_{HPt}$ = 25 Hz, 6H, NCH_3), 2.27 (s, $^3J_{HPt}$ = 18 Hz, 6H, NCH_3). ^{19}F NMR (C_6D_6, 282.2 MHz, 23 °C): δ −93.6 (s, $^2J_{FPt}$ = 426 Hz, CF_2), −81.0 (s, $^3J_{FPt}$ = 65 Hz, CF_3).

(TMEDA)Pt(*n*-C_3F_7)(CH_3)I_2 (13). Addition of hexanes (15 mL) to a mixture of (TMEDA)Pt(*n*-C_3F_7)(CH_3) (0.200 g, 0.404 mmol) and I_2 (0.103 g, 0.406 mmol) followed by stirring for 3 h gave an orange-brown precipitate in a purple solution. The solid was collected on a glass frit and washed repeatedly with hexanes. Yield: 0.249 g, 82%. Anal. Calcd for $C_{10}H_{19}F_7I_2N_2Pt$: C, 16.03; H, 2.56; N, 3.74. Found: C, 16.13; H, 2.46; N, 3.65. ^{1}H NMR ($CDCl_3$, 300 MHz, 23 °C): δ 2.87 (t, $^2J_{HF}$ = 2.1 Hz, 3H, $^2J_{HPt}$ = 71.7 Hz, PtMe), 2.87−3.05 (m, 4H, CH_2), 3.29 (s, 6H, $^3J_{HPt}$ = 18.0 Hz, NMe), 3.31 (s, 6H, $^3J_{HPt}$ = 12.6 Hz, NMe). ^{19}F NMR ($CDCl_3$, 282.2 MHz, 23 °C): δ −116.0 (s, β-CF_2), −79.4 (t, $^4J_{FF}$ = 13 Hz, $^4J_{FPt}$ = 15 Hz, CF_3), −48.8 (q, $^4J_{FF}$ = 13 Hz, $^2J_{FPt}$ = 251 Hz, α-CF_2). Crystals for the structure determination were obtained from CH_2Cl_2/heptane as dark red blocks.

(TMEDA)Pt(*n*-C_3F_7)I (14). Addition of moist CH_2Cl_2 (15 mL) to a mixture of (TMEDA)Pt(C_3F_7)(CH_3)I_2 (0.194 g, 0.259 mmol) and $AgBF_4$ (0.111 g, 0.570 mmol) gave a pale yellow precipitate in a colorless solution. The mixture was stirred for 30 min, and then a solution of NaI (0.20 g, excess) in H_2O (5 mL) was added and the resultant slurry stirred for 90 min. The organic layer was separated, dried over anhydrous Na_2SO_4, and filtered through Celite to give pale yellow solution. Removal of solvent in vacuo afforded a yellow solid. Yield: 0.146 g, 93%. Anal. Calcd for $C_9H_{16}F_7IN_2Pt$: C, 17.80; H, 2.66; N, 4.61. Found: C, 17.95; H, 2.63; N, 4.59. ^{1}H NMR ($CDCl_3$, 300 MHz, 23 °C): δ 2.62−2.76 (m, 4H, CH_2), 2.92 (brs, 6H, $^3J_{HPt}$ = 17.4 Hz, NMe), 2.98 (br s, 6H, $^3J_{HPt}$ = 45.0 Hz, NMe). ^{1}H NMR (toluene-d_8, 500 MHz, −70 °C): δ 0.53 (br d, J_{HH} = 12 Hz, CH_2), 0.72 (br d, J_{HH} = 12 Hz, 1H, CH_2), 1.66 (br t, J_{HH} = 12 Hz, 1H, CH_2), 1.93 (br t, J_{HH} = 12 Hz, 1H, CH_2), 1.98 (br s, 3H, NMe), 2.19 (br s, 3H, NMe), 2.28 (br s, 3H, NMe), 2.81 (br s, 3H, NMe). ^{19}F NMR ($CDCl_3$, 282.2 MHz, 23 °C): δ −113.0 (br s, β-CF_2), −79.8 (t, $^3J_{FPt}$ = 11 Hz, CF_3). ^{19}F NMR (toluene-d_8, 470.4 MHz, −60 °C): δ −114.6 (d, $^2J_{FF}$ = 283 Hz, β-CF), −110.9 (d, $^2J_{FF}$ = 283 Hz, β-CF), −94.2 (d, $^2J_{FF}$ = 262 Hz, α-CF), −78.9 (m, CF_3), −64.4 (d, $^2J_{FF}$ = 262 Hz, α-CF).

[(TMEDA)Pt(*n*-C_3F_7)(OH_2)]O_3SCF_3 (17). Addition of CF_3SO_3H (0.020 mL, 0.226 mmol) to a solution of (TMEDA)Pt(*n*-C_3F_7)(CH_3) (0.100 g, 0.202 mmol) in CH_2Cl_2 (15 mL) gave a pale yellow solution, which was stirred for 2 h. Removal of volatiles in vacuo gave a white solid, which was washed with $CHCl_3$. Yield: 0.050 g, 38%. Anal. Calcd for $C_{10}H_{18}F_{10}N_2O_4PtS$: C, 18.55; H, 2.80; N, 4.30. Found: C, 18.73; H, 2.72; N, 4.31. ^{1}H NMR (acetone-d_6, 300 MHz, 23 °C): δ 2.83 (s, 6H, NMe), 3.04 (s, 6H, NMe), 3.02−3.15 (m, 4H, CH_2). ^{19}F NMR (acetone-d_6, 282.2 MHz, 23 °C): δ −119.8 (s, $^3J_{FPt}$ = 48 Hz, β-CF_2), −99.8 (s, $^2J_{FPt}$ = 260 Hz, α-CF_2), −80.6 (t, $^3J_{FF}$ = 11 Hz, CF_3), −79.3 (s, SO_3CF_3).

(TMEDA)Pt(*n*-C_3F_7)H (18). Addition of EtOH (10 mL) to a mixture of (TMEDA)Pt(*n*-C_3F_7)I (0.092 g, 0.152 mmol) and $NaBH_4$ (0.2 g, excess) and stirring for 1 h gave a colorless suspension. Removal of volatiles followed by extraction into toluene and filtration through Celite gave a colorless solution, which was reduced in vacuo to a white solid. Yield: 0.070 g, 96%. Anal. Calcd for $C_9H_{17}F_7N_2Pt$: C, 22.46; H, 3.56; N, 5.82. Found: C, 22.24; H, 3.43; N, 5.76. ^{1}H NMR (C_6D_6, 300 MHz, 23 °C): δ −20.96 (br s, 1H, $^1J_{HPt}$ = 1734 Hz, PtH), 1.36−1.48 (m, 4H, CH_2), 2.12 (s, 6H, $^3J_{HPt}$ = 32.1 Hz, NMe), 2.29 (s, 6H, $^3J_{HPt}$ = 18.3 Hz, NMe). ^{19}F NMR (C_6D_6, 282.2 MHz, 23 °C): δ −119.9 (d, $^4J_{FH}$ = 4 Hz, $^3J_{FPt}$ = 233 Hz, β-CF_2), −88.2 (q, $^4J_{FF}$ = 10.5 Hz, $^2J_{FPt}$ = 402 Hz, α-CF_2), −78.3 (t, $^4J_{FF}$ = 10.5 Hz, $^4J_{FPt}$ = 60 Hz, CF_3). ^{19}F NMR (CD_2Cl_2, 470.4 MHz, −75 °C): δ −118.7 (d, $^2J_{FF}$ = 279 Hz, $^3J_{FPt}$ = 235 Hz, β-CF), −117.8 (d, $^2J_{FF}$ = 279 Hz, $^3J_{FPt}$ = 238 Hz, β-CF), −88.5 (br d, $^2J_{FF}$ = 276 Hz, $^2J_{FPt}$ = 328 Hz, α-CF), −87.1 (br d, $^2J_{FF}$ = 276 Hz, $^2J_{FPt}$ = 384 Hz, α-CF), −77.2 (t, $^4J_{FF}$ = 10 Hz, CF_3). Crystals for the structure determination were grown from Et_2O/heptane as colorless prisms.

(DPPE)Pt(*n*-C_3F_7)(CH_3) (19). A solution of (TMEDA)Pt(*n*-C_3F_7)Me (1.00 g, 2.02 mmol) and DPPE (0.808 g, 2.03 mmol) in toluene (10 mL) was heated under reflux for 3 h. The resultant colorless solution was reduced in vacuo to a white solid, which was collected on a glass frit and washed with EtOH and then hexanes. Yield: 1.47 g, 93%. Anal. Calcd for $C_{30}H_{27}F_7P_2Pt$: C, 46.34; H, 3.50. Found: C, 46.20; H, 3.45. ^{1}H NMR ($CDCl_3$, 300 MHz, 23 °C): δ 0.63 (t, $^3J_{HP}$ = 7.2 Hz, 3H, $^2J_{HPt}$ = 84 Hz, PtMe), 2.11−2.24 (m, 4H, CH_2), 7.37−7.51 (m, 12H, Ph), 7.62−7.69 (m, 8H, Ph). ^{19}F NMR ($CDCl_3$, 282.2 MHz, 23 °C): δ −119.5 (s, $^3J_{FPt}$ = 84 Hz, β-CF_2), −88.1 (m, $^2J_{FPt}$ = 366 Hz, α-CF_2), −80.1 (t, $^4J_{FF}$ = 10 Hz, $^4J_{FPt}$ = 27 Hz, CF_3). ^{31}P{^{1}H} NMR ($CDCl_3$, 121.4 MHz, 23 °C): δ 45.6 (t, $^3J_{PF}$ = 28.8 Hz, $^1J_{PPt}$ = 2101 Hz), 49.1 (t, $^3J_{PF}$ = 33.4 Hz, $^1J_{PPt}$ = 1779 Hz).

(DPPE)Pt(*n*-C_3F_7)OT_f (20). Addition of CF_3SO_3H (0.046 g, 0.307 mmol) to a solution of (DPPE)Pt(*n*-C_3F_7)(CH_3) (0.200 g, 0.257 mmol) in CH_2Cl_2 (15 mL) and stirring for 16 h gave a pale yellow solution, which was reduced in vacuo to a yellow oil. Dissolution in CH_2Cl_2 and filtration through Celite, followed by addition of toluene and removal of the CH_2Cl_2 in vacuo, gave a white precipitate, which was collected on a glass frit and washed with toluene. Yield: 0.225 g, 94%. Crystals suitable for X-ray diffraction analysis were grown by slow evaporation of a CH_2Cl_2 solution. (dppe)Pt(C_3F_7)OT_f (**20**): Anal. Calcd for $C_{30}H_{24}F_{10}P_2O_3PtS$: C, 39.53; H, 2.65. Found: C, 39.60; H, 2.61. ^{1}H NMR (CD_2Cl_2, 300 MHz, 23 °C): δ 2.04−2.55 (m, 4H, CH_2), 7.50−7.68 (m, 12H, Ph), 7.74−7.85 (m, 8H, Ph). ^{19}F NMR (CD_2Cl_2, 282.2 MHz, −20 °C): δ −118.4 (s, β-CF_2), −91.8 (s, $^2J_{FPt}$ = 325 Hz, α-CF_2), −78.9 (s, CF_3), −76.5 (br, s, SO_3CF_3). ^{31}P{^{1}H} NMR (CD_2Cl_2, 121.4 MHz, −30 °C): δ 36.1 (m, $^1J_{PPt}$ = 4651 Hz), 46.0 (br t, $^3J_{PF}$ = 29 Hz, $^1J_{PPt}$ = 1963 Hz). [(dppe)Pt(C_3F_7)(OH_2)]OT_f (**21**): ^{1}H NMR (CD_2Cl_2, 300 MHz, −20 °C): δ 2.12−2.21 (m, 2H, CH_2), 2.35−2.45 (m, 2H, CH_2), 7.51−7.77 (m, 20H, Ph). ^{19}F NMR (CD_2Cl_2, 282.2 MHz, −20 °C): δ −118.9 (s, β-CF_2), −96.1 (s, $^2J_{FPt}$ = 310 Hz, α-CF_2), −78.6 (br, s, CF_3), −77.6 (s, O_3SCF_3). ^{31}P{^{1}H} NMR (CD_2Cl_2, 121.4 MHz, −40 °C): δ 34.5 (td, $^3J_{PF}$ = 13.0 Hz, $^2J_{PP}$ = 5.3 Hz, $^1J_{PPt}$ = 4409 Hz), 46.8 (br t, $^3J_{PF}$ = 29 Hz, $^1J_{PPt}$ = 1969 Hz).

(DPPE)Pt(*n*-C_3F_7)I (22). Method A. To a solution of (DPPE)Pt(*n*-C_3F_7)OT_f (0.123 g, 0.132 mmol) in moist CH_2Cl_2 was added a solution of NaI (0.19 g, excess) in H_2O (5 mL). The resultant colorless emulsion was stirred for 16 h. Separation of the organic layer followed by drying over $MgSO_4$ and filtration through Celite gave a colorless solution. Removal of solvent in vacuo gave a white solid, which was washed with EtOH and hexanes. Yield: 0.114 g, 97%. Anal. Calcd for $C_{29}H_{24}F_7IP_2Pt$: C, 39.16; H, 2.70. Found: C, 38.92; H, 2.74. ^{1}H NMR ($CDCl_3$, 300 MHz, 23 °C): δ 2.03−2.15 (m, 4H, CH_2), 7.45−7.57 (m, 12H, Ph), 7.72−7.79 (m, 8H, Ph). ^{19}F NMR ($CDCl_3$, 282.2 MHz, 23 °C): δ −114.8 (s, $^3J_{FPt}$ = 56 Hz, β-CF_2), −80.2 (t, $^4J_{FF}$ = 9.5 Hz, CF_3), −79.4 (m, $^2J_{FPt}$ = 366 Hz, α-CF_2). ^{31}P{^{1}H} NMR ($CDCl_3$, 121.4 MHz, 23 °C): δ 40.3 (t, $^3J_{PF}$ = 29 Hz, $^1J_{PPt}$ = 1785 Hz), 42.5 (td, $^3J_{PF}$ = 28 Hz, $^2J_{PP}$ = 4.5 Hz, $^1J_{PPt}$ = 3806 Hz).

Method B. A suspension of ((DPPE)Pt(*n*-C_3F_7)(CH_3) (0.100 g, 0.129 mmol) and I_2 (0.033 g, 0.130 mmol) in hexanes (15 mL) was stirred for 16 h. The resultant white precipitate was collected by filtration and then recrystallized from CH_2Cl_2/EtOH. Yield: 0.088 g, 77%.

(DPPE)Pt(*n*-C_3F_7)H (23). To a solution of (DPPE)Pt(*n*-C_3F_7)I (0.114 g, 0.128 mmol) in CH_2Cl_2 (15 mL) was added a solution of $NaBH_4$ (0.15 g, excess) in EtOH (5 mL) and the resultant suspension stirred for 30 min. The solid residue was extracted into Et_2O and filtered through Celite. Removal of solvent in vacuo gave a white solid, which was washed with EtOH and hexanes. Yield: 0.092 g, 94%. Anal. Calcd for $C_{29}H_{25}F_7P_2Pt$: C, 45.62; H, 3.27. Found: C, 45.35; H, 3.26. ^{1}H NMR ($CDCl_3$, 300 MHz, 23 °C): δ −2.81 (ddtt, $^2J_{HP}$ = 189 Hz, $^2J_{HP}$ = 15 Hz, $^3J_{HF}$ = 8.0 Hz, $^4J_{HF}$ = 7.0 Hz, 1H, $^1J_{PtH}$ = 1209 Hz, PtH), 2.20−2.40 (m, 4H, CH_2), 7.38−7.45 (m, 12H, Ph), 7.60−7.70 (m, 4H, Ph), 7.75−85 (m, 4H, Ph). ^{19}F NMR ($CDCl_3$, 282.2 MHz, 23 °C): δ −121.1 (dd, $^4J_{FP}$ = 7 Hz, $^4J_{FH}$ = 7 Hz, $^3J_{FPt}$ = 152 Hz, β-CF_2), −83.3 (ddqd, $^3J_{FP}$ = 33 Hz, $^3J_{FP}$ = 32 Hz, $^4J_{FF}$ = 10 Hz, $^3J_{FH}$ = 8 Hz, $^2J_{FPt}$ = 379 Hz, α-CF_2), −79.2 (t, $^4J_{FF}$ = 10 Hz, $^4J_{FPt}$ = 40 Hz, CF_3). ^{31}P{^{1}H} NMR ($CDCl_3$, 121.4 MHz, 23 °C): δ 49.0 (t, $^3J_{PF}$ = 33 Hz, $^1J_{PtP}$ = 2043 Hz), 50.7 (tt, $^3J_{PF}$ = 32 Hz, $^4J_{PF}$ = 7 Hz, $^1J_{PtP}$ = 1812 Hz). The latter resonance has the large coupling to the hydride resonance and is consequently that of the phosphorus *trans* to H.

Crystallographic Structural Determinations. Crystal, data collection, and refinement parameters are collected in Table 1. The systematic absences in the diffraction data are uniquely consistent for the reported space groups. Compound **23** crystallized with two independent molecules in the asymmetric unit. The structures were solved using direct methods, completed by subsequent difference Fourier syntheses, and refined by full-matrix least-squares procedures. DIFABS absorption corrections were applied to all structures. All nonhydrogen atoms were refined with anisotropic displacement coefficients, and hydrogen atoms were treated as idealized contributions.

All software and sources of the scattering factors are contained in the SHELXTL (5.10) program library.

Acknowledgment. R.P.H. is grateful to the National Science Foundation and to the Petroleum Research Fund, administered by the American Chemical Society for generous financial support.

Supporting Information Available: Atomic fractional coordinates, bond distances and angles, and anisotropic thermal parameters for complexes **6a**, **9a**, **9b**, **10**, **13**, **18**, **19**, **20**, and **23** are available free of charge via the Internet at http://pubs.acs.org.

OM010424H